J|A|C|S COMMUNICATIONS

Published on Web 02/05/2010

Chemical Solution Deposition of Epitaxial Carbide Films

Guifu Zou,*,† Haiyan Wang,‡ Nathan Mara,† Hongmei Luo,§ Nan Li,† Zengfeng Di,† Eve Bauer,† Yongqiang Wang,† Thomas McCleskey,† Anthony Burrell,† Xinghang Zhang,‡ Michael Nastasi,† and Quanxi Jia*,†

Los Alamos National Laboratory, Los Alamos, New Mexico 87545, Texas A&M University, College Station, Texas 77843, and New Mexico State University, Las Cruces, New Mexico 88003

Received December 3, 2009; E-mail: gfzou@lanl.gov; qxjia@lanl.gov

Transition-metal carbides have hardness similar to that of diamond but are far cheaper than diamond. Besides the mechanical hardness, carbides also show other unique properties, such as high-temperature stability, corrosion and oxidation resistance, and low electrical resistivity.[1] These properties make them very attractive for applications in wear coatings, passivation layers, and high-temperature electronic devices.[2] To realize the strong hardness, high stability, and low electrical resistivity, high-quality epitaxial carbide films are generally required.[3] To date, very limited physical and chemical vapor deposition methods have been used to grow carbide (e.g., TiC, VC, TaC, etc.) films on different substrates.[4] Chemical solution deposition for the growth of films, on the other hand, provides advantages such as low cost, easy setup, and coating of large areas. Here we report the growth of epitaxial carbide films such as TiC, VC, and TaC on Al_2O_3 substrates by a chemical solution deposition (i.e., polymer-assisted deposition) method initially developed for the growth of metal oxide films.[5] These epitaxial carbide films exhibit structural and physical properties similar to the films grown by physical and chemical vapor deposition techniques. In this communication, we mainly discuss the epitaxial TiC films synthesized by such a solution deposition method.

The X-ray diffraction (XRD) patterns of a TiC film on *c*-plane Al_2O_3 are shown in Figure 1, including (a) the $\theta-2\theta$ scan, (b) the (111) rocking curve, and (c) ϕ scans of (200) TiC and (104) Al_2O_3. As can be seen from the $\theta-2\theta$ scan, a well-defined (111) TiC reflection is observed. The appearance of only the (111) diffraction peak indicates that the TiC film is preferentially oriented with respect to the substrate surface. A value of 0.4° for the full width at half-maximum (fwhm) of the (111) rocking curve (Figure 1b) shows the good crystallinity of the film. As shown in Figure 1c, the six peaks of the (111)-oriented TiC film on *c*-plane Al_2O_3 indicate the in-plane alignment between the film and the substrate as well. An average fwhm value of 1.2° for the TiC film, in comparison with the value of 0.7° for the single-crystal Al_2O_3 substrate, indicates the film to have good epitaxial quality. The in-plane alignment between the film and the substrate can be understood by considering the crystal structures of both TiC and Al_2O_3. Cubic TiC has a space group of $Fm\bar{3}m$. Six peaks in the ϕ scan are expected for epitaxial (111) TiC films. Meanwhile, rhombohedral Al_2O_3 has a space group of $R\bar{3}m$. Three peaks in the ϕ scan are expected for the *c*-plane Al_2O_3 substrate. A 30° rotation with respect to the Al_2O_3 is anticipated by considering the lattice match between the film and the substrate, since such an alignment gives a small lattice mismatch of less than 2.7%. On the basis of Figure 1a,c, the heteroepitaxial relationships between the TiC film

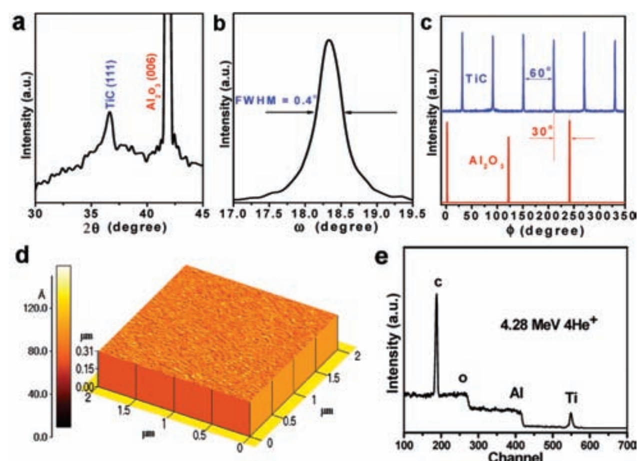

Figure 1. XRD patterns, surface morphology, and element analysis of a TiC film on a *c*-plane Al_2O_3 substrate: (a) $\theta-2\theta$ scan; (b) rocking curve from the (111) reflection; (c) ϕ scans from the (200) and (104) reflections of the film and substrate, respectively; (d) AFM image; (e) NRBS spectrum.

and the Al_2O_3 substrate can be described as $(111)_{TiC}\|(006)_{Al_2O_3}$ and $[100]_{TiC}\|[120]_{Al_2O_3}$. In addition, the lattice parameter of the epitaxial TiC film is 4.371 Å. In comparison with the lattice parameter of bulk cubic TiC (a = 4.327 Å), the epitaxial film is under compressive strain. This is reasonable in view of the $d_{[111]}$ of TiC (2.46 Å) and $d_{[120]}$ of Al_2O_3 (2.35 Å). We note that other epitaxial carbide films such as VC and TaC were also grown on Al_2O_3 substrates using a similar process, and their XRD results are shown in Figure S1 in the Supporting Information.

Figure 1d shows an atomic force microscopy (AFM) image of the TiC film. The film is uniform and has no detectable microcracks. The grain size and root-mean-square surface roughness of the film are 50 and 3.5 nm, respectively. Scanning electron microscopy (SEM) images across a large area give similar results, as shown in Figure S2. The chemical composition of the film was estimated by nuclear resonance backscattering spectroscopy (NRBS) using a 4.28 MeV $^4He^+$ beam with a detector angle of 167°. With such a resonance technique, the scattering cross section for carbon can be nearly 30 times higher than the Rutherford value at a typical 2 MeV beam energy. This makes it possible to detect carbon signals that otherwise would be buried in the O and Al signals from the Al_2O_3 substrate. By using a known carbon standard, one can accurately determine the metal-to-carbon ratio in the carbide film. As shown in the NRBS spectrum (Figure 1e), no impurities were observed in the TiC film. An average Ti/C atomic ratio of 1:1.1 is close to the 1:1 stoichiometic ratio in TiC. A slightly higher carbon concentration can be attributed to the extra gaseous carbon source used in our experiment and possible residual polymer used in the precursor materials.

† Los Alamos National Laboratory.
‡ Texas A&M University.
§ New Mexico State University.

10.1021/ja9102315 © 2010 American Chemical Society

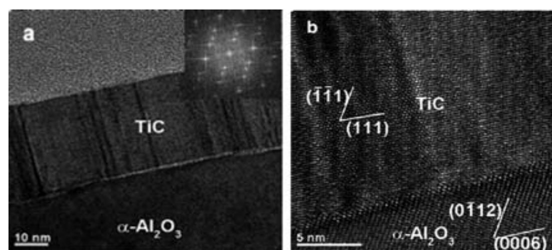

Figure 2. (a) TEM and (b) HRTEM images of a TiC film on a *c*-plane Al_2O_3 substrate. The inset in (a) shows the corresponding FFT pattern.

The extremely smooth surface morphology and highly epitaxial nature of the TiC film are further confirmed by the bright-field cross-section transmission electron microscopy (TEM) and high-resolution TEM (HRTEM) images shown in Figure 2. The thickness of the TiC film is in the range 40−50 nm. The HRTEM images, taken from the [1$\bar{1}$0] zone axis of TiC, show the film to be epitaxial with [111] normal to the substrate surface. Importantly, the interface between the film and the substrate is smooth and shows no indication of intermixing. The corresponding fast Fourier transform (FFT) pattern taken from the interface (Figure 2a inset) confirms the epitaxial growth of the TiC film on the *c*-plane Al_2O_3 substrate, as evidenced by the distinct diffraction spots in the film and the substrate. The epitaxial relationship between the film and the substrate determined from the FFT patterns is consistent with that determined from the XRD patterns. More careful observation of the HRTEM image reveals that there is a bright line at the interface of the TiC film and the *c*-plane Al_2O_3. It should be noted that this was not observed when the TiC film was deposited on *r*-plane Al_2O_3. However, there are obvious twin microstructures for the TiC film on *r*-plane Al_2O_3 (Figure S3). It is known that misfit dislocations and twins can release the lattice strain in the heteroepitaxial growth of films.[6,7] Our experimental results suggest that different relaxations take place for the TiC films grown on the *c*- and *r*-plane Al_2O_3 substrates.

The mechanical hardness of TiC films prepared by our method is similar to those of films deposited by other techniques. As shown in the top panel of Figure 3a, the hardness is in the range 19.53−22.93 GPa throughout the penetration depth. Our TiC film possesses an average hardness of ∼21.27 GPa, which is as good as the value of ∼20 GPa for TiC films formed by physical vapor deposition.[4b,8] In addition, the Young's modulus of the TiC films (bottom panel of Figure 3a) has values in the range 440−396 GPa, which is higher than that of reported TiC films,[4b] although it is lower than that of bulk TiC, which has a value of 450 GPa. It has been reported that a stoichiometric deviation (Ti/C) can decrease the hardness.[9]

Our epitaxial TiC film exhibits a semiconductive resistivity versus temperature characteristic with a resistivity of ∼372 $\mu\Omega$ cm at room temperature. As shown in Figure 3b, the resistivity of TiC increased almost exponentially with decreasing temperature at temperatures lower than 25 K. It should be noted that the resistivity of our epitaxial TiC film is still ∼5 times larger than that of bulk TiC (70 $\mu\Omega$ cm). In addition, the semiconductive resistivity versus temperature behavior of the epitaxial TiC film does not agree with first-principles calculations.[10] In general, the electrical conduction for a given material depends on the defects and impurities.[11] The crystallinity and grain boundary can also significantly alter the resistivity versus temperature behavior of conductive films.[12] In particular, it has been shown that carbon impurities and grain-boundary scattering can increase the resistivity[13] or lead to semiconductive behavior[14] of conductive films. Our NRBS results

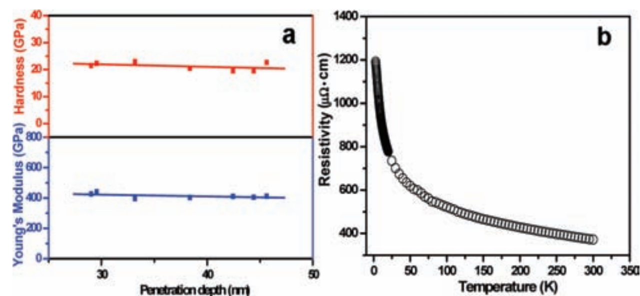

Figure 3. Characteristics of a TiC film on a *c*-plane Al_2O_3 substrate: (a) hardness (top panel) and Young's modulus (bottom panel) as a function of penetration depth; (b) resistivity vs temperature characteristic.

do show extra carbon in our TiC films due to either the use of ethylene gas or polymer in the precursor to prepare the TiC films. Similar semiconductive resistivity versus temperature behavior was also reported for TiC films deposited by vapor deposition.[15]

In summary, epitaxial carbide films have been successfully grown on Al_2O_3 substrates by a chemical solution deposition technique for the first time. The desired crystal and microstructures of the films have been confirmed by XRD and HRTEM. The epitaxial relationships between the TiC film and *c*-plane Al_2O_3 substrate are $(111)_{TiC}||(006)_{Al_2O_3}$ and $[100]_{TiC}||[120]_{Al_2O_3}$. The TiC films possess hardness and Young's modulus as large as 21.27 and 413 GPa, respectively. The epitaxial TiC film shows a semiconductive resistivity versus temperature characteristic with a resistivity of ∼372 $\mu\Omega$ cm at room temperature.

Acknowledgment. This work was supported by the U.S. Department of Energy through the LANL/LDRD Program and the Center for Integrated Nanotechnologies. H.W. thanks the NSF for funding (NSF0709831 and NSF0846504).

Supporting Information Available: Synthesis and characterization of carbide films. This material is available free of charge via the Internet at http://pubs.acs.org.

References

(1) Pierson, H. O. *Handbook of Refractory Carbides and Nitrides: Properties, Characteristics, Processing and Applications*; Noyes Publications: Westwood, NJ, 1996.
(2) Chaddha, A.; Parsons, J.; Kruaval, G. B. *Appl. Phys. Lett.* **1995**, *66*, 760.
(3) Luo, H.; Jain, M.; McCleskey, T.; Bauer, E.; Burrell, A.; Jia, Q. X. *Adv. Mater.* **2007**, *19*, 3604.
(4) (a) Cheon, J.; Dubois, L.; Girolami, G. S. *J. Am. Chem. Soc.* **1997**, *119*, 6814. (b) Wang, J.; Li, W.; Li, H. *J. Mater. Sci.* **2000**, *35*, 2689. (c) Norin, L.; Hogberg, H.; Lu, J.; Jansson, U.; Malm, J. *Appl. Phys. Lett.* **1998**, *73*, 2754. (d) Liao, M.; Gotoh, Y.; Tsuji, H.; Ishikawa, J. *J. Vac. Sci. Technol., A* **2005**, *23*, 1379. (e) Chang, Y.; Wu, J.; Chang, P.; Chiu, H. *J. Mater. Chem.* **2003**, *13*, 365. (f) Vispute, R.; Hullavarad, S.; Luykx, A.; Young, D.; Dhar, S.; Venkatesan, T.; Jones, K.; Zheleva, T.; Ervin, M.; Derenge, M. *Appl. Phys. Lett.* **2007**, *90*, 241917. (g) Girolami, G.; Jensen, J.; Allocca, C.; Kaloyeros, A.; Williams, W. *J. Am. Chem. Soc.* **1987**, *109*, 1579.
(5) Jia, Q. X.; McCleskey, T.; Burrell, A.; Lin, Y.; Collis, G.; Wang, H.; Li, A.; Foltyn, S. *Nat. Mater.* **2004**, *3*, 529.
(6) Luo, H.; Wang, H.; Bi, Z.; Zou, G.; McCleskey, T.; Burrell, A.; Bauer, E.; Hawley, M.; Wang, Y.; Jia, Q. X. *Angew. Chem., Int. Ed.* **2009**, *48*, 1490.
(7) Cao, L.; Lee, T.; Johnson, R.; Zegenhage, J. *Phys. Rev. B* **2002**, *65*, 113402.
(8) Buinno, N.; Narayan, J.; Srivatsa, A. R. *Appl. Phys. Lett.* **1989**, *54*, 1519.
(9) Andriewski, A.; Spivak, I. *Strength of Refractory Compounds and Related Materials*; Metallurgy: Tcheljabinsk, Russia, 1989; p 28.
(10) Tsetseris, L.; Pantelides, S. T. *Acta Mater.* **2008**, *56*, 2864.
(11) Toth, L. *Transition Metal Carbides and Nitrides*; Academic Press: New York, 1971.
(12) Jia, Q. X.; Chu, F.; Adams, C.; Wu, X.; Hawley, M.; Cho, J.; Findikoglu, A.; Foltyn, S.; Smith, J.; Mitchell, T. *J. Mater. Res.* **1996**, *11*, 2263.
(13) Inoue, S.; Wada, Y.; Koterazawa, K. *Vacuum* **2000**, *59*, 735.
(14) Hollander, L. E. *J. Appl. Phys.* **1961**, *32*, 996.
(15) Munster, A.; Sagel, K.; Schlamp, G. *Nature* **1954**, *174*, 1154.

JA9102315